Acta Pharmacologica Sinica

www.nature.com/aps

ARTICLE

The vascular endothelial growth factor trap aflibercept induces vascular dysfunction and hypertension via attenuation of eNOS/NO signaling in mice

Zhi-chao Dong[1,2], Ming-ming Wu[1], Yun-long Zhang[2], Qiu-shi Wang[1], Chen Liang[1], Xiao Yan[2], Lei-xin Zou[2], Chen Chen[2], Xiao Han[2], Bo Zhang[2] and Zhi-ren Zhang[1]

Aflibercept, as a soluble decoy vascular endothelial growth factor receptor, Which has been used as a first-line monotherapy for cancers. Aflibercept often causes cardiovascular toxicities including hypertension, but the mechanisms underlying aflibercept-induced hypertension remain unknown. In this study we investigated the effect of short-term and long-term administration of aflibercept on blood pressure (BP), vascular function, NO bioavailability, oxidative stress and endothelin 1 (ET-1) in mice and cultured endothelial cells. We showed that injection of a single-dose of aflibercept (18.2, 36.4 mg/kg, iv) rapidly and dose-dependently elevated BP in mice. Aflibercept treatment markedly impaired endothelial-dependent relaxation (EDR) and resulted in NADPH oxidases 1 (NOX1)- and NADPH oxidases 4 (NOX4)-mediated generation of ROS, decreased the activation of protein kinase B (Akt) and endothelial nitric oxide synthase (eNOS) concurrently with a reduction in nitric oxide (NO) production and elevation of ET-1 levels in mouse aortas; these effects were greatly attenuated by supplementation of *L*-arginine (*L*-arg, 0.5 or 1.0 g/kg, bid, ig) before aflibercept injection. Similar results were observed in *L*-arg-pretreated cultured endothelial cells, showing markedly decreased ROS accumulation and AKT/eNOS/NO signaling impairment induced by aflibercept. In order to assess the effects of long-term aflibercept on hypertension and to evaluate the beneficial effects of *L*-arg supplementation, we administered these two drugs to WT mice for up to 14 days (at an interval of two days). Long-term administration of aflibercept resulted in a sustained increase in BP and a severely impaired EDR, which are associated with NOX1/NOX4-mediated production of ROS, increase in ET-1, inhibition of AKT/eNOS/NO signaling and a decreased expression of cationic amino acid transporter (CAT-1). The effects caused by long-term administration were greatly attenuated by *L*-arg supplementation in a dose-dependent manner. We conclude that aflibercept leads to vascular dysfunction and hypertension by inhibiting CAT-1/AKT/eNOS/NO signaling, increasing ET-1, and activating NOX1/NOX4-mediated oxidative stress, which can be suppressed by supplementation of *L*-arg. Therefore, *L*-arg could be a potential therapeutic agent for aflibercept-induced hypertension.

Keywords: aflibercept; hypertension; endothelial dysfunction; superoxide production; endothelin 1; cationic amino acid transporter-1; *L*-arginine; cultured endothelial cells

Acta Pharmacologica Sinica (2021) 42:1437–1448; https://doi.org/10.1038/s41401-020-00569-1

INTRODUCTION

Angiogenesis plays a critical role in tumor growth and the development of metastasis. Vascular endothelial growth factor (VEGF) and its receptors (VEGFRs) are important inducers of these processes. There are two major tyrosine kinase receptors for VEGF signals, namely, VEGFR1 (Flt-1) and VEGFR2 (Flk-1) [1]. Upon stimulation by VEGF, VEGFR1 and VEGFR2 are activated, initiating a tyrosine kinase signaling cascade that promotes cell survival, proliferation, migration, and differentiation into mature blood vessels during the development of cancer. Thus, the use of VEGF–VEGFR inhibitors (VEGFIs) could be a promising strategy for the treatment and management of various cancers. Indeed, VEGFIs are now considered first-line monotherapies for some types of cancers. One such VEGFI is aflibercept, a soluble decoy VEGFR constructed by fusing the Ig domains of VEGFR1 and VEGFR2 with the Fc region of human IgG1. It strongly binds to VEGF and placental growth factor thereby blocking activation of the cognate VEGFR1/2 [2, 3], which is an established treatment for several tumor types.

Unfortunately, clinical studies have revealed that VEGFIs are associated with cardiovascular toxicity, especially hypertension [4]. Preexisting hypertension, smoking, older age (>65 years), and excess weight are important risk factors for the development of VEGFI-induced hypertension [5]. Several mechanisms have been proposed, including vascular remodeling, endothelial dysfunction, renal injury, activation of the renin-angiotensin system, and capillary rarefaction

[1]Departments of Clinical Pharmacy and Cardiology, Harbin Medical University Cancer Hospital, Institute of Metabolic Disease, Heilongjiang Academy of Medical Science, Key Laboratories of Education Ministry for Myocardial Ischemia Mechanism and Treatment, Harbin 150000, China and [2]Department of Cardiology, The First Affiliated Hospital, Dalian Medical University, Dalian 116011, China
Correspondence: Bo Zhang (dalianzhangbo@yahoo.com) or Zhi-ren Zhang (zhirenz@yahoo.com)

Received: 15 July 2020 Accepted: 29 October 2020
Published online: 10 December 2020

[6, 7]. Moreover, endothelial nitric oxide synthase (eNOS)/nitric oxide (NO) signaling, oxidative stress, and endothelin 1 (ET-1) are also involved in the development of hypertension during antiangiogenic therapy [8]. It has been reported that 42.4% and 17.4% of aflibercept-treated patients develop hypertension and hypertensive crisis, respectively [9, 10]. However, the mechanism involved in aflibercept-induced hypertension remains unknown.

In this study, we investigated the effect of short-term and long-term administration of aflibercept on blood pressure (BP), vascular function, NO bioavailability, oxidative stress and ET-1 in mice and cultured endothelial cells. We also evaluated the beneficial effect of *L*-arginine (*L*-arg) supplementation on aflibercept-induced adverse effects. Our results demonstrated that aflibercept predominantly inhibited protein kinase B (AKT)/eNOS signaling and cationic amino acid transporter-1 (CAT-1), which reduced NO levels, and increased superoxide, and ET-1 production, thereby leading to impaired vasodilatation and BP elevation. The results also suggest that *L*-arg could be a potential therapeutic drug for treating aflibercept-induced hypertension.

MATERIALS AND METHODS

Animal experiments

Several studies suggest that estrogen affects vascular function and hypertension [11, 12], and these physiological effects of estrogen might generate bias to the experimental results [13]. Therefore, male C57BL/6 mice aged 8–10 weeks were purchased from Vital River Laboratory Animal Technology Co. Ltd (Beijing, China). All animal experiment protocols were approved by the Animal Care and Use Committee of Harbin Medical University. The procedures conformed to the *Guide for the Care and Use of Laboratory Animals* published by the US National Institutes of Health.

We purchased aflibercept (Zaltrap, 100 mg/4 mL) from Sanofi S.A. (Paris, France). The dose of aflibercept was selected based upon the practice guide for dose conversion between mice and humans [14]. Since the recommended dose of aflibercept for patients is 4 mg/kg via intravenous infusion, the calculated optimal dose of aflibercept is 36.4 mg/kg for mice. To further confirm whether the aflibercept-induced increase in BP occurred in a dose-dependent manner, relatively low dose of aflibercept (18.2 mg/kg) was also used in our experiments. A single dose of 18.2 mg/kg or 36.4 mg/kg aflibercept (defined as short-term administration) or five doses of 18.2 mg/kg or 36.4 mg/kg aflibercept at an interval of 2 days (defined as long-term administration) was inravenously administered to the mice [15, 16]. Angiotensin II (Ang II) was infused at a dose of 490 ng·kg^{-1}·min^{-1} using osmotic mini-pumps (Alzet, model 1002; Durect, Cupertino, USA) as a positive control. To investigate whether *L*-arg could prevent aflibercept-induced hypertension, 3 days before administration of aflibercept the mice were orally gavaged with *L*-arg (0.5 or 1.0 g/kg) twice daily until the end of experiments, according to previously reported doses [17, 18]. To investigate whether *L*-arg has a therapeutic effect on aflibercept-induced hypertension, *L*-arg (1.0 g/kg) was given twice daily for 7 days after aflibercept injection.

Cell culture

Primary human umbilical vein endothelial cells (HUVECs) were isolated from freshly obtained human umbilical cords by 0.1% collagenase and 0.1% trypsin digestion, as described previously [19], and grown in endothelial cell medium (ScienCell Research Laboratories, Carlsbad, CA, USA) supplemented with 1% endothelial cell growth factor, 10% fetal bovine, and penicillin/streptomycin (100 U/mL). In all experiments, we used cells between the fourth and tenth passages in vitro. We treated HUVECs with saline or aflibercept (50 nM) for 24 h, the concentration of aflibercept used in HUVEC experiments was based on previous studies [20, 21]. To investigate whether *L*-arg could prevent against oxidative stress and decrease in the production of NO induced by aflibercept, we preincubated HUVECs with *L*-arg (0.5 mM) for 6 h, and then aflibercept (50 nM) for 24 h [15, 22, 23]. Once the cells reached confluence, the culture medium was removed, and the cells were washed twice (1 min each) with phosphate buffered saline solution (PBS), pH 7.4, at 4 °C, lysed with RIPA buffer or PBS and collected after scraping. The samples were either immediately analyzed or stored at −80 °C until analysis.

Blood pressure monitoring

BP was measured by a tail-cuff system (SoftronBP-98A; Softron, Tokyo, Japan) [24], and during the measurement, ten individual readings were obtained. The highest and lowest readings were discarded, and the average of the remaining eight readings was used. A radiotelemetry probe catheter (HD-X100, O.D 0.4 mm, Data Science International Inc.) was implanted into the aortic arch via the left carotid artery as previously described [25]. Following 1 week of recovery, the mice, which were housed in individual cages, were placed above the telemetric receivers with output to a computer. BP was recorded by scheduled sampling for 10 s every 1 min (Dataquest LabPRO Acquisition System version 3.01, Data Sciences International, St. Paul, MN, USA) [26].

Histopathology

Aortic sections were fixed in formalin, embedded in paraffin, sectioned (5 μm), and stained with hematoxylin and eosin (H&E) and Masson's trichrome reagent as described previously [24]. The cryosections were stained with dihydroethidium (DHE, 1 μM in PBS) for 30 min at 37 °C; and red DHE fluorescence was detected using a Nikon Labophot 2 microscope (Nikon, Tokyo, Japan). Digital images were taken at ×100 or ×200 magnification, and analyzed by Image-Pro Plus 3.0 (Nikon, Tokyo, Japan).

Functional analysis by myography

Intact aortas were gently isolated from mice, stripped of adventitial fat under a dissecting microscope, and then cut into 4 mm segments. The aortic rings were gently mounted on force transducers (DMT, Multi Wire Myography System—620M, Denmark), and the organ chambers were filled with Krebs solution (pH 7.2–7.4, containing 120 mM NaCl, 5.5 mM KCl, 2.5 mM $CaCl_2$, 1.2 mM $MgCl_2{\cdot}6H_2O$, 1.2 mM Na_2HPO_4, 20 mM $NaHCO_3$, 0.03 mM EDTA-Na_2, and 10 mM glucose) and continuously gassed with a mixture of 95% O_2 and 5% CO_2 at a temperature of 37 °C. Each ring was stretched to 3 mN and then allowed to equilibrate for 60 min before the experiment was initiated. After the 60 min stabilization period, KPSS (pH 7.38–7.40, containing 5.248 g NaCl, 4.473 g KCl, 0.244 g $MgCl_2{\cdot}6H_2O$, 0.277 g $CaCl_2$, 2.0 g glucose, and 1.915 g HEPES in 1000 mL H_2O) was added to the chambers and washed out with Krebs solution until producible maximal contraction was achieved. After stimulation by phenylephrine, vascular responses to increasing concentrations of acetylcholine (ACh) (1×10^{-9} M to 1×10^{-4} M) and sodium nitroprusside (SNP) (1×10^{-9} M to 1×10^{-5} M) were recorded; percent relaxation was calculated as previously described [26, 27].

Western blot analysis

For Western blot analysis, total proteins were extracted from snap-frozen aortic tissue or cultured cells by using RIPA buffer and protease inhibitor cocktail (Thermo Fisher Scientific Co.). Protein concentrations were determined by the BCA Assay Kit. Equal amounts of total protein (50 μg) were separated by 8%–10% SDS-PAGE and transferred to polyvinylidene difluoride (PVDF) membranes with the Bio-Rad Western blotting system. PVDF membrane (Bio-Rad) was probed with primary antibodies, including AKT, p-AKT (Ser473), p-eNOS (Ser1177), eNOS, CAT-1, nicotinamide adenine dinucleotide phosphate (NADPH) oxidases 1 and 4 (NOX1 and NOX4) (Cell Signaling Technology and Abcam, 1:800–1:1000 dilution), and GAPDH (Cell Signaling Technology, 1:3000 dilution) at 4 °C overnight and then with horseradish peroxidase-conjugated secondary

antibodies (1:2500) for 1 h at room temperature (22–24 °C). All blots were developed by using a chemiluminescence system, and signal intensities were analyzed with a Gel-Pro 4.5 Analyzer (MediaCybernetics, USA) as previously described [28]. GAPDH was used as the internal standard to control for protein quantity.

Biochemical measurements

The levels of ET-1 and NO in the serum and aorta were detected using ELISA kits (Nanjing Jiancheng Bioengineering Institute, Nanjing, China). The concentrations of renin, Ang II, aldosterone, dopamine, noradrenaline in the serum and nitrotyrosine in the aortas were measured with the ELISA kits (Cloud-Clone Corp, Wuhan, China). The concentration of *L*-arg in HUVECs was measured with an ELISA kit (Abcam, USA). The manufacturer's instructions were strictly followed when performing the test and interpreting the results.

DAF-FM and DHE fluorescence staining

HUVECs were grown on microscope coverslips, and intracellular NO levels in cells incubated with 5 μM of 3-amino-4-aminomethyl-2′, 7′-difluorescein (DAF-FM) (Molecular Probes, Thermo Fisher, USA) were determined according to the method described previously [29]. Briefly, the treated cells were incubated with 5 mM DAF-FM for 25 min and then washed twice with PBS. The Fluorescence was observed in fixed cells with a laser confocal scanning microscope (Olympus, Fluoview 1000, Japan). Excitation at 488 nm and emission at 510 nm were used.

Dihydroethidium (DHE), was used to measure ROS levels in HUVECs. The cells were incubated with 5 μM DHE in phenol red-free medium for 1 h. Fluorescence microscopy was also used to visualize differences in fluorescence intensities at the end of 1 h of incubation with DHE [30]. The signal density was analyzed by ImageJ software (a Java-based imaging processing program, National Institute of Health, USA). NO and superoxide production are presented as the fold change in fluorescence signal compared with that in the control group.

Chemical reagents

Unless otherwise noted, all reagents used in this study were purchased from Sigma Aldrich.

Statistical analysis

All values are presented as the means ± SEMs and were analyzed with SPSS 22.0. Comparisons were made by one-way ANOVA (S-N-K and Bonferroni's method) or independent *t*-test as appropriate. Values of $P < 0.05$ were considered statistically significant.

RESULTS

Short-term aflibercept treatment increases blood pressure and impairs vascular function in mice

To investigate the effect of aflibercept on BP, we treated WT mice with a single dose of aflibercept at 18.2 or 36.4 mg/kg and monitored BP from days 1 to 4 using both noninvasive tail-cuff measurements and radio telemetry. The data showed that hypertension was dose-dependently induced in aflibercept-treated mice compared with saline-treated control [31] (Fig. 1a). Systolic BP and mean arterial pressure (MAP) levels rapidly increased on day 1, peaked on day 2, and then gradually decreased on days 3 and 4 (Fig. 1a and Supplementary Fig. 1a). Radiotelemetry measurements showed the same patterns in SBP in mice after high-dose aflibercept administration (36.4 mg/kg; Fig. 1b–d). These results therefore indicate that aflibercept induces an acute increase in BP.

To test whether aflibercept affects vascular relaxation, we evaluated ex vivo aortic function in WT mice at different times (day 1, 2, 3, 4) after high-dose aflibercept (36.4 mg/kg) treatment. Intact aortas were isolated, and the concentration–relaxation relationships for ACh or SNP were analyzed. The data showed that ACh-mediated vasodilatation was markedly impaired by high-dose aflibercept (36.4 mg/kg) on day 1, this impairment peaked on days 2 and 3, and ACh-mediated vasodilatation was partially recovered on day 4 (Fig. 1e). However, aflibercept only mildly affected endothelium-independent vasodilatation in response to the SNP at all time points (Fig. 1f). Moreover, H&E staining revealed no aortic wall thickening in high-dose aflibercept (36.4 mg/kg)-treated mice compared with saline-treated control mice (Fig. 1g). These results suggest that aflibercept predominantly impairs endothelium-dependent relaxation (EDR) after short-term aflibercept treatment.

Short-term aflibercept treatment results in NOX1/NOX4-mediated ROS accumulation and attenuates AKT/eNOS/NO signaling in the mouse aorta

To elucidate the mechanism by which aflibercept elevates BP, we first examined ROS production, which is known to mediate the perturbation of vascular tone [32]. Consistent with the changes in BP patterns (Fig. 1a–d), aflibercept at a high dose (36.4 mg/kg) significantly increased the levels of ROS and peroxynitrite ($ONOO^-$) formation in aortas, as reflected by increases in the relative DHE intensity and nitrotyrosine levels (Fig. 2a, b). Moreover, the protein expression levels of NOX1 and NOX4 were significantly increased by application of high-dose aflibercept, in a similar pattern as the changes in BP (Fig. 2c). We next measured the levels of NO in the mice treated with aflibercept. After treatment, NO levels in serum and aortic tissues were significantly reduced on day 1, this decrease peaked on days 2 and 3, and NO levels were partially recovered on day 4 (Fig. 2d, e). Moreover, the levels of serum ET-1 were markedly increased in aflibercept-treated mice compared with saline-treated control at all time points (Fig. 2f).

Aflibercept is known to block the VEGFR/AKT/eNOS signaling pathway [33]. We then next examined its effect on these signaling mediators in these pathways. Immunoblotting showed that aflibercept treatment did not alter the expression levels of VEGFR1 and VEGFR2 (Fig. 2g), but did markedly reduce the phosphorylation of Akt (Ser473) and eNOS (Ser1177), compared with saline-treated mice at all time points (Fig. 2h). This effect paralleled with the change patterns in NO in aflibercept-treated mice (Fig. 2d, e).

L-arg supplementation prevents aflibercept-induced hypertension, impairment of endothelial-dependent relaxation, ROS accumulation, and reduction in NO production

We next examined whether *L*-arg, the substrate of eNOS and the main precursor of NO, could prevent aflibercept-induced hypertension. The mice were randomly divided into five groups and were, respectively, administered by saline (control), *L*-arg ($1.0\ g \cdot kg^{-1} \cdot d^{-1}$), aflibercept (36.4 mg/kg), and aflibercept plus two different doses (0.5 or $1.0\ g \cdot kg^{-1} \cdot d^{-1}$) of *L*-arg twice daily. The *L*-arg administration started 3 days before applying aflibercept and ended at day 4. While *L*-arg had no effect on BP, the aflibercept-induced increase in systolic BP and MAP were greatly attenuated by $0.5\ g \cdot kg^{-1} \cdot d^{-1}$ *L*-arg and were completely reversed by $1.0\ g \cdot kg^{-1} \cdot d^{-1}$ *L*-arg (Fig. 3a and Supplementary Fig. 1b).

We next assessed whether *L*-arg ($1.0\ g \cdot kg^{-1} \cdot d^{-1}$) protects against the high-dose aflibercept-induced reduction in NO production and impairment of EDR in mice. The data show that NO levels in the aorta were significantly decreased and that EDR was severely impaired in the aflibercept-treated group compared with the saline-treated control group; these effects were markedly reversed by *L*-arg supplementation (Fig. 3b, c). Consistently, neither aflibercept nor *L*-arg affected endothelium-independent vasodilatation in response to SNP (Fig. 3d). Moreover, aflibercept-induced elevation of aortic ROS levels (as indicated by DHE staining) (Fig. 3e, f) and the increased levels of ET-1 (Fig. 3g) were reversed by $1.0\ g \cdot kg^{-1} \cdot d^{-1}$ *L*-arg supplementation.

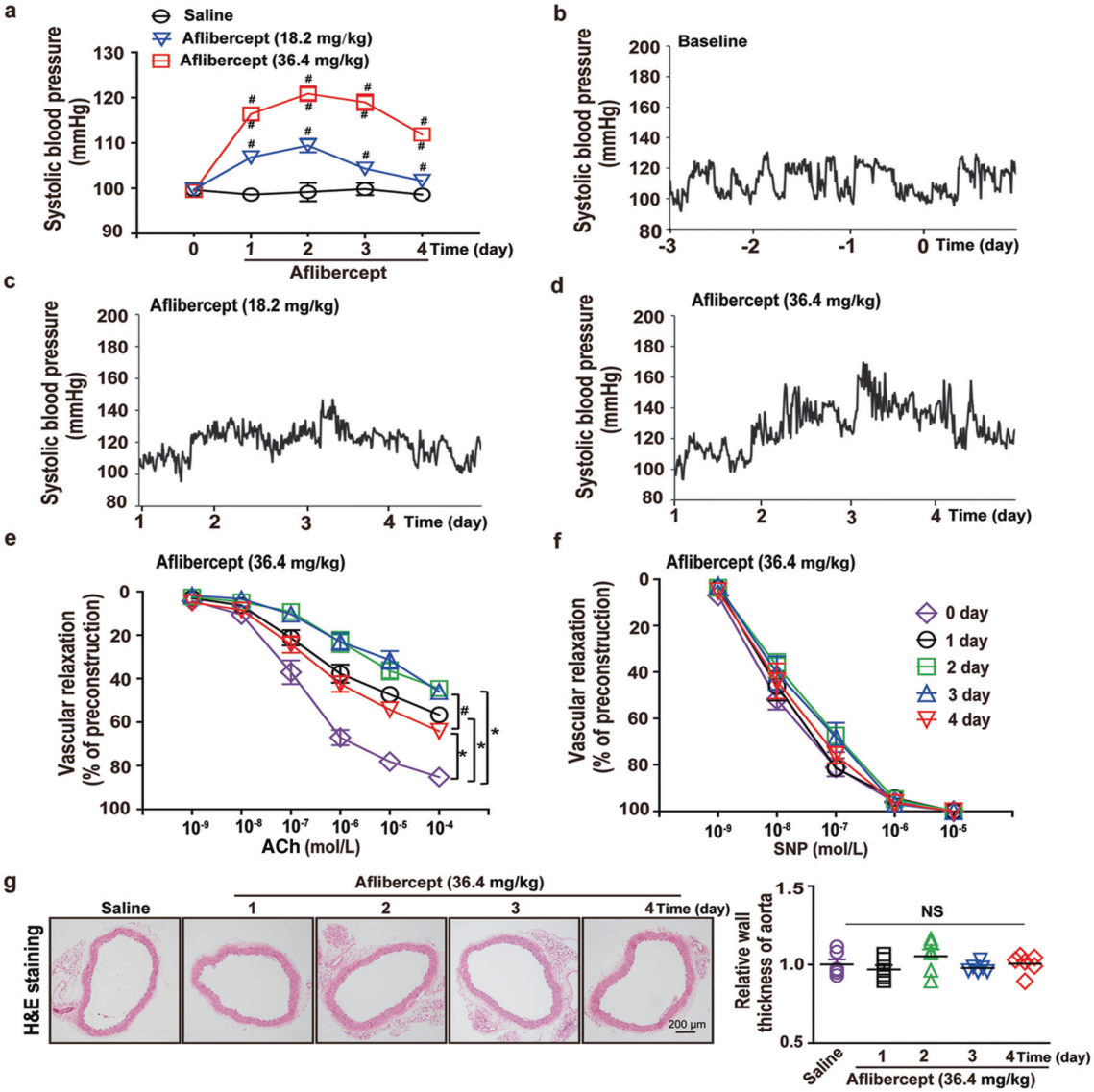

Fig. 1 A single dose of aflibercept leads to an acute increase in SBP and impairment of vascular function. a SBP was measured by the noninvasive tail-cuff method before and after treatment with a single dose of saline or aflibercept ($n = 8$; $^{*}P < 0.05$ versus the saline group; $^{\#}P < 0.05$ versus the low-dose aflibercept group). **b**–**d** Representative SBP recordings from WT mice 3 days before aflibercept treatment as a baseline (**b**) and 1–4 days after infusion of a single dose of aflibercept at 18.4 mg/kg (**c**) or 36.4 mg/kg (**d**) using radiotelemetric BP measurements ($n = 6$). **e**, **f** Dose-response curves for endothelium-dependent (**e**) and endothelium-independent relaxation (**f**) at different times (1–4 days) after treatment with 36.4 mg/kg aflibercept ($n = 8$; $^{*}P < 0.05$ versus the saline group; $^{\#}P < 0.05$ versus the 4th day after aflibercept treatment group). **g** Representative images of H&E staining of thoracic aortas. Wall thickness in each group ($n = 6$). The data are presented as the mean ± SEM; *n* represents the number of samples or mice; NS no significant difference; SBP systolic blood pressure; ACh acetylcholine; SNP sodium nitroprusside.

L-arg prevents aflibercept-induced accumulation of ROS and impairment of AKT/eNOS/NO signaling in cultured endothelial cells

To identify the mechanisms by which *L*-arg protects against aflibercept-induced vascular dysfunction and hypertension, HUVECs were treated with *L*-arg (0.5 mM), and then stimulated with aflibercept (50 nM) for 24 h. While *L*-arg did not affect NO levels, aflibercept significantly reduced NO levels (as indicated by DAF-FM staining) compared with the saline-treated control group. Aflibercept-induced reduction in NO levels was markedly reversed by the application of *L*-arg (Fig. 4a). Moreover, while *L*-arg had a modest effect on ROS, the aflibercept-induced increase in ROS (as indicated by DHE staining) was markedly reduced by *L*-arg (Fig. 4b). Interestingly, aflibercept-induced increase in the expression levels of NOX1 and NOX4 was significantly blunted by *L*-arg (Fig. 4c, d). Moreover, the dramatic aflibercept-induced decrease in the levels of phosphorylated Akt (Ser473) and eNOS (at Ser1177) was also rescued by *L*-arg (Fig. 4c, e). Surprisingly, the expression levels of CAT-1 and the intracellular concentration of *L*-arg were significantly decreased by aflibercept in HUVECs (Fig. 4c, f, g). The effects of aflibercept on CAT-1 and the intracellular concentration of *L*-arg were greatly attenuated by *L*-arg (Fig. 4f, g).

L-arg can prevent and treat aflibercept-induced hypertension and vascular dysfunction in mice

To evaluate the long-term effect of aflibercept on BP, the mice were randomly assigned into different groups: the mice, respectively, were treated with saline, *L*-arg (1.0 g· kg^{-1}· d^{-1}), aflibercept (18.2 mg/kg),

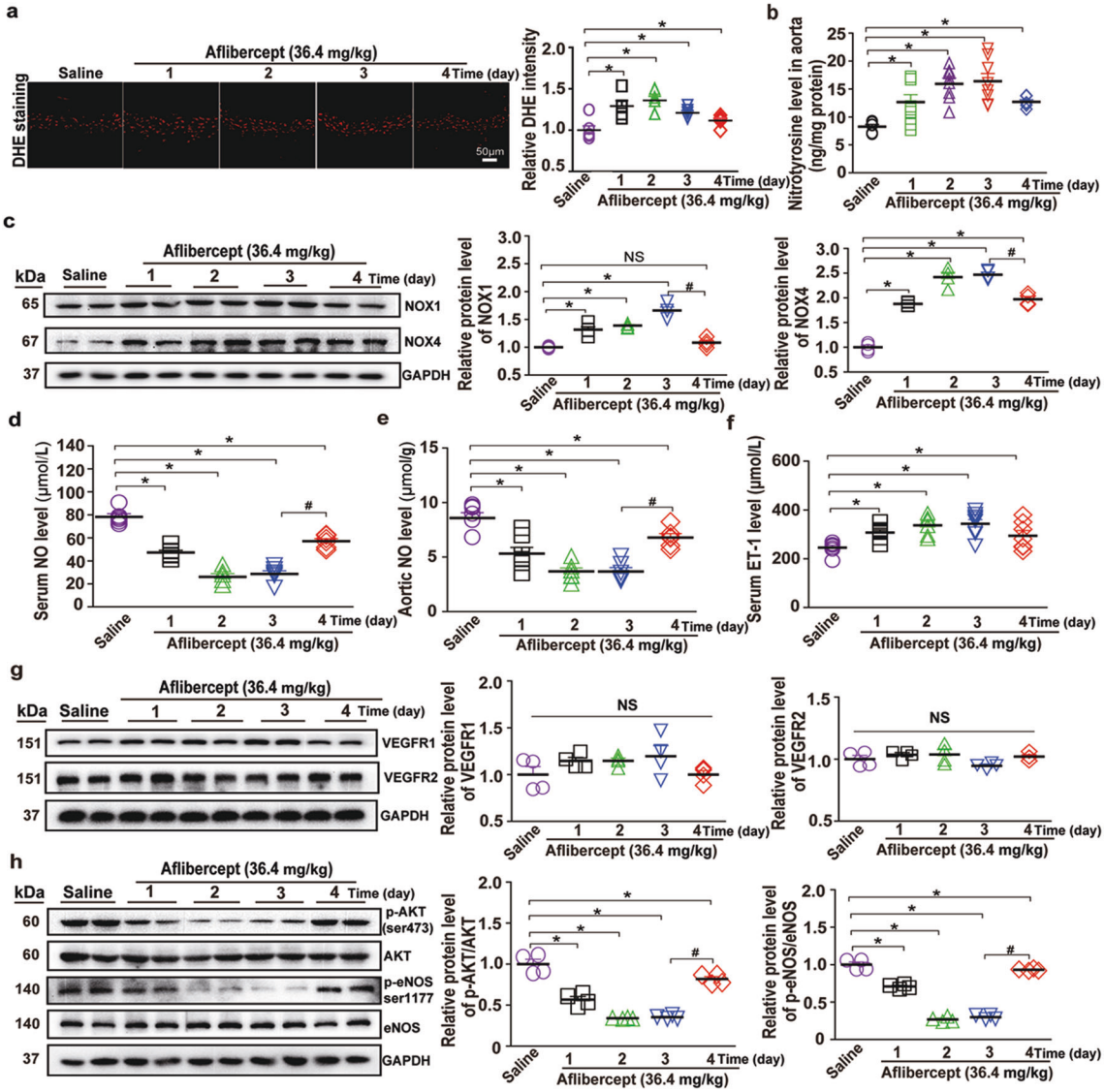

Fig. 2 A single dose of aflibercept results in NOX1/NOX4-mediated ROS accumulation and impairs AKT/eNOS/NO signaling. **a** Representative images of DHE staining of aortic segments after injection of a single dose of 36.4 mg/kg aflibercept, and DHE fluorescence intensity from the data representing ROS levels on days 1–4 after aflibercept injection ($n = 5$; scale bar; 50 μm; $^*P < 0.05$ versus the saline group). **b** Nitrotyrosine was assessed as an index of peroxynitrite ($ONOO^-$) formation in aorta ($n = 7$–8; $^*P < 0.05$ versus saline group). **c** Immunoblotting analysis of NOX1 and NOX4 protein expression in the aorta before and after injection of 36.4 mg/kg aflibercept and protein abundance from the experiments was shown ($n = 4$; $^*P < 0.05$ versus the saline group; $^\#P < 0.05$ versus the 3rd day after aflibercept treatment group). **d**, **e** Aflibercept significantly reduced NO levels in serum and aortic tissues ($n = 6$ or 7; $^*P < 0.05$ versus the saline group; $^\#P < 0.05$ versus the 4th day after aflibercept treatment group). **f** Aflibercept significantly increased ET-1 levels in serum ($n = 6$ or 7; $^*P < 0.05$ versus the saline group). **g** Representative immunoblots showing VEGFR1 and VEGFR2 protein expression in the aorta; Protein expression levels of VEGFR1 and VEGFR2 before and after aflibercept injection ($n = 4$). **h** Representative immunoblots showing p-AKT (Ser473), AKT, p-eNOS (Ser1177), and eNOS expression in the aorta, and quantification of protein levels from the data were shown ($n = 4$; $^*P < 0.05$ versus the saline group; $^\#P < 0.05$ versus the 3rd day after aflibercept treatment group). The data are presented as the mean ± SEM; *n* represents number of samples or mice; NS no significant difference; Akt protein kinase B; p-Akt phosphorylated Akt; eNOS endothelial nitric oxide synthase; p-eNOS phosphorylated eNOS.

aflibercept (36.4 mg/kg), aflibercept (36.4 mg/kg) plus *L*-arg at two different doses (0.5 and 1.0 g· kg^{-1} ·d^{-1}), or Ang II infusion (served as a positive control) for up to 14 days.

The tail-cuff measurement data showed that aflibercept-treated mice displayed significant elevations in SBP and MAP compared with control group, in a similar pattern as that induced by Ang II infusion (Fig. 5a and Supplementary Fig. 1c). Aflibercept-induced increase in SBP and MAP was significantly prevented by low-dose *L*-arg (0.5 g· kg^{-1} ·d^{-1}) and was completely reversed by high-dose *L*-arg (1.0 g ·kg^{-1} ·d^{-1}), suggesting that preapplication of *L*-arg could prevent aflibercept-induced hypertension in mice, in a dose-dependent manner (Fig. 5a and Supplementary Fig. 1c). The SBP data generated from radio-telemetry measurements showed the same results as those derived from tail-cuff measurements (Fig. 5b–g). We next examined whether *L*-arg could decrease aflibercept-induced hypertension using a protocol, in which the mice were administered aflibercept for 7 days followed by high dose of *L*-arg. The data showed that the significant increases in SBP and MAP induced by aflibercept were significantly inhibited by *L*-arg (1.0 g· kg^{-1} ·d^{-1}), suggesting that *L*-arg has a therapeutic effect on aflibercept-induced hypertension. Furthermore, long-term injection of low dose aflibercept led to an increase in BP with

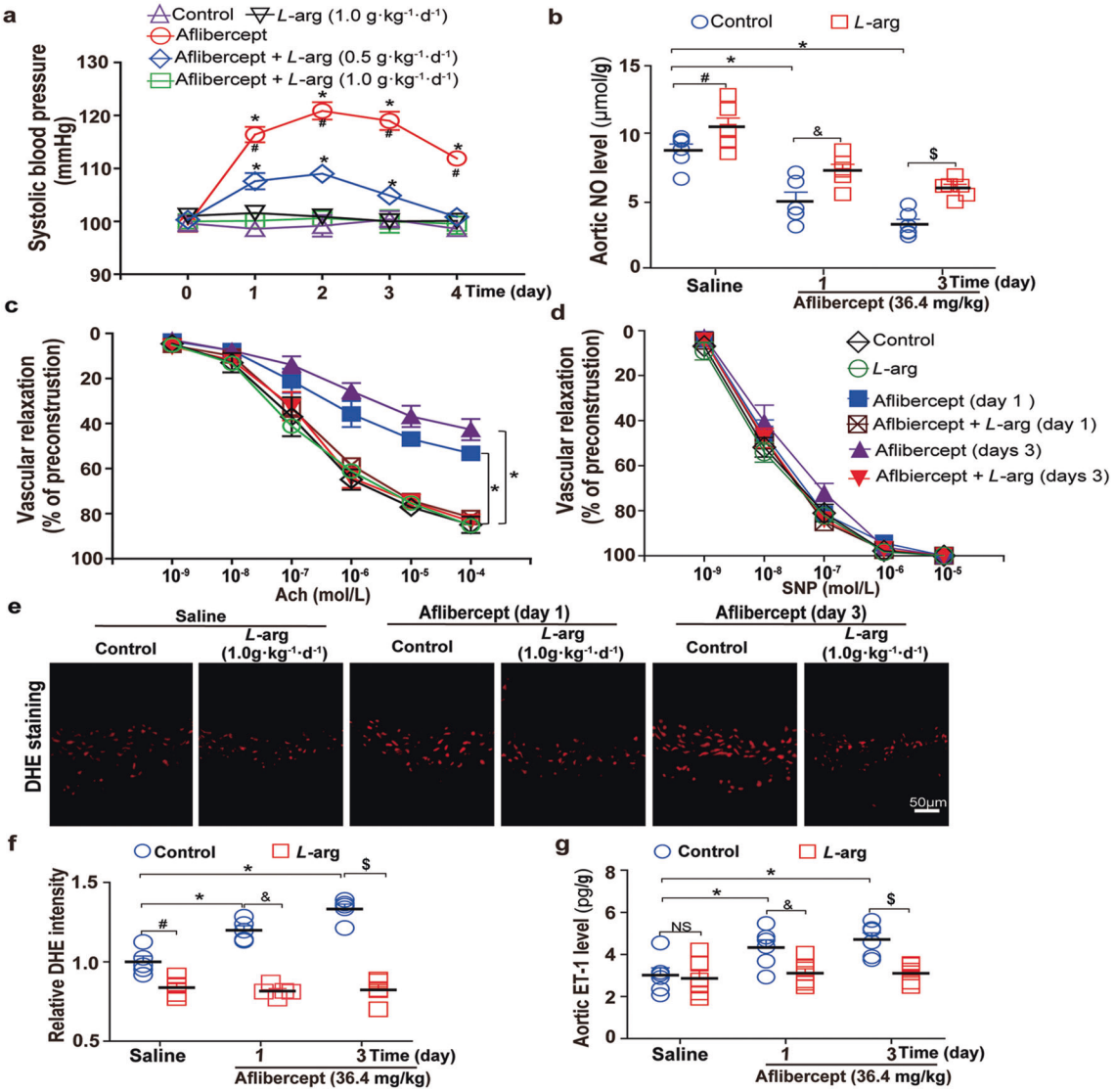

Fig. 3 ***L*-arg supplementation prevents hypertension, impairment of EDR, ROS accumulation, and reduction in NO production induced by a single dose of aflibercept. a** SBP was measured by the noninvasive tail-cuff method in mice treated with saline or *L*-arg (0.5 or 1.0 g· kg^{-1} ·d^{-1}) before and after injection of a single dose of 36.4 mg/kg aflibercept ($n = 6$; *$P < 0.05$ versus the saline group; $^{\#}P < 0.05$ versus the low-dose *L*-arg group). **b** Following injection of a single dose of aflibercept, NO levels in the aortic tissues were measured using a nitric oxide assay kit in the presence or absence of *L*-arg (1.0 g· kg^{-1}· d^{-1}) on days 1 and 3 ($n = 6$; *$P < 0.05$ versus the saline group; $^{\#}P < 0.05$ versus the *L*-arg group; $^{\&}P < 0.05$ versus the 1st day after aflibercept + *L*-arg treatment group; $^{\$}P < 0.05$ versus the 3rd day after aflibercept + *L*-arg treatment group). **c**, **d** Dose-response curves for endothelium-dependent (**c**) and endothelium-independent relaxation (**d**) were constructed on days 1 and 3 after 36.4 mg/kg aflibercept injection in the presence or absence of *L*-arg (1.0 g· kg^{-1} ·d^{-1}) ($n = 7$ or 8; *$P < 0.05$ versus the saline group). **e**, **f** Representative images of DHE staining of aortic segments (**e**) and DHE fluorescence intensity data demonstrating that aflibercept-induced ROS accumulation was reversed by *L*-arg (**f**) ($n = 5$; *$P < 0.05$ versus the saline group; $^{\#}P < 0.05$ versus the *L*-arg group; $^{\&}P < 0.05$ versus the 1st day after aflibercept + *L*-arg treatment group; $^{\$}P < 0.05$ versus the 3rd day after aflibercept + *L*-arg treatment group). **g** ET-1 levels in aortic tissues were measured after administration of a single dose of aflibercept on days 1 and 3 in the absence or presence of *L*-arg ($n = 6$; *$P < 0.05$ versus the saline group; $^{\&}P < 0.05$ versus the 1st day after aflibercept + *L*-arg treatment group; $^{\$}P < 0.05$ versus the 3rd day after aflibercept + *L*-arg treatment group). The data are presented as the mean ± SEM; *n* represents the number of samples or mice; NS no significant difference.

the similar pattern as high-dose aflibercept, albeit to a lesser extent (Fig. 6a and Supplementary Fig. 1d).

Moreover, EDR in response to ACh was severely impaired in high-dose aflibercept-treated mice compared with saline-treated control mice, and this impairment was markedly prevented by low-dose *L*-arg and was reversed by high-dose *L*-arg (Fig. 5h). Aflibercept treatment did not significantly affect endothelium-independent vasodilatation in response to SNP (Fig. 5i). We further tested whether long-term injcetion of low-dose aflibercept (18.2 mg/kg) impaired EDR in the mouse aorta. The data showed that while low-dose aflibercept injection did not affect endothelium-independent relaxation, it resulted in a slight, but significant impairment of EDR (Fig. 6b, c). Consistently, we found that long-term injection of high-dose aflibercept led to a dramatic impairment of EDR in the mouse aorta; importantly, this preexisting aflibercept-induced impairment of EDR was dramatically improved by high-dose *L*-arg (1.0 g· kg^{-1} ·d^{-1}) (Fig. 6b); whereas endothelium-independent vasodilation was not signifi-

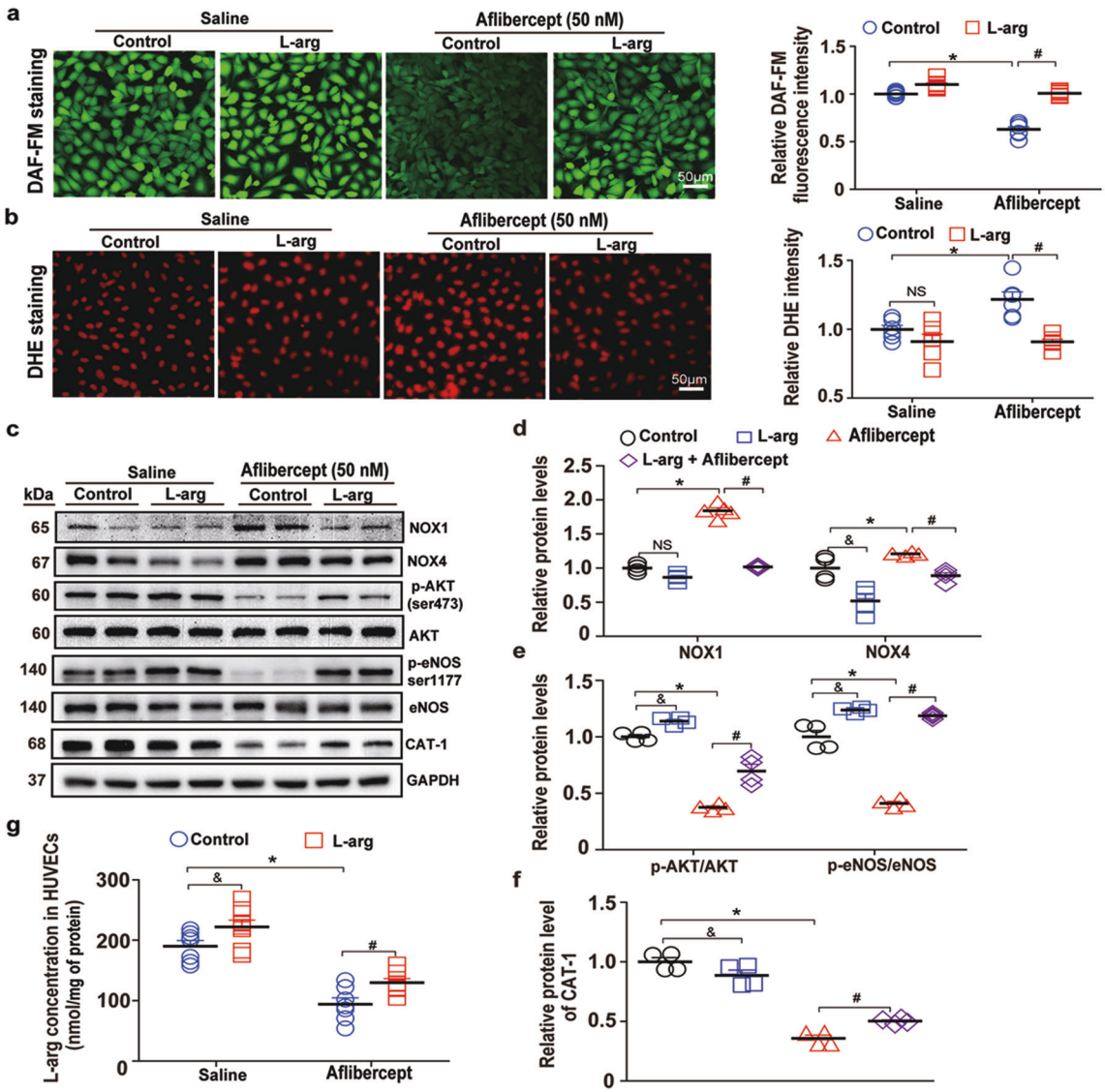

Fig. 4 ***L*-arg prevents against aflibercept-induced ROS accumulation and impairment of AKT/eNOS/NO in cultured endothelial cells.** **a** Green fluorescence observed by confocal microscopy in cells preloaded with DAF-FM representing intracellular NO levels, and integrative fluorescence per image demonstrating that the aflibercept-induced reduction in NO levels was rescued by *L*-arg ($n = 6$; $^{*}P < 0.05$ versus the saline group; $^{\#}P < 0.05$ versus the aflibercept group). **b** Representative DHE staining of HUVECs and DHE fluorescence intensity data demonstrating that aflibercept-induced ROS accumulation was reserved by *L*-arg in each group ($n = 6$; $^{*}P < 0.05$ versus the saline group; $^{\#}P < 0.05$ versus the aflibercept group). **c**–**f** Representative immunoblots showing NOX1, NOX4, p-AKT (Ser473), AKT, p-eNOS (Ser1177), eNOS, and CAT-1 expression in HUVECs (**c**) and quantification of protein expression levels from the data shown in (**d**–**f**) ($n = 4$; $^{*}P < 0.05$ versus the saline group; $^{\&}P < 0.05$ versus the *L*-arg group; $^{\#}P < 0.05$ versus the aflibercept group). **g** The intracellular *L*-arg concentration in HUVECs was measured by the *L*-Arginine Assay Kit, and the data showed that the aflibercept-induced decrease in intracellular *L*-arg was greatly attenuated by extracellular *L*-arg supplementation ($n = 6$; $^{*}P < 0.05$ versus the saline group; $^{\&}P < 0.05$ versus the *L*-arg group; $^{\#}P < 0.05$ versus the aflibercept group). The data are presented as the mean ± SEM; *n* represents the number of samples or mice.

cantly affected (Fig. 6c).

L-arg attenuates oxidative stress and the reduction in eNOS/NO signaling induced by long-term application of aflibercept

After aflibercept administration, the isolated mice aortas were stained with DHE to assess the levels of ROS under different experimental conditions. The data showed that ROS levels were significantly increased in long-term aflibercept-treated mice compared to both control or *L*-arg administered mice; this aflibercept-induced accumulation of ROS was significantly attenuated by 0.5 g/kg *L*-arg and reversed by 1.0 g/kg *L*-arg (Fig. 7a). Furthermore, the long-term aflibercept-induced reduction of p-eNOS (Ser1177) (Fig. 7b) and NO levels (Fig. 7c) was markedly elevated by *L*-arg, in a dose-dependent manner. It is noteworthy that the aortic p-eNOS and NO levels were slightly but significantly increased by 1.0 g/kg *L*-arg compared to the control (Fig. 7b, c). Hypertension causes structural remodeling of the arterial walls; therefore, we further assessed whether long-term aflibercept treatment induced aortic remodeling. The histological staining (H&E and Masson's staining) data showed that long-term aflibercept treatment did not affect aortic-wall thickness and fibrotic area in mice (Fig. 7d–f).

DISCUSSION

The major findings of the present study are as follows: (1) aflibercept administration leads to NOX1/NOX4-mediated ROS accumulation; (2) aflibercept treatment results in an increase in ET-1 levels; (3) aflibercept impairs AKT/eNOS/NO signaling and EDR

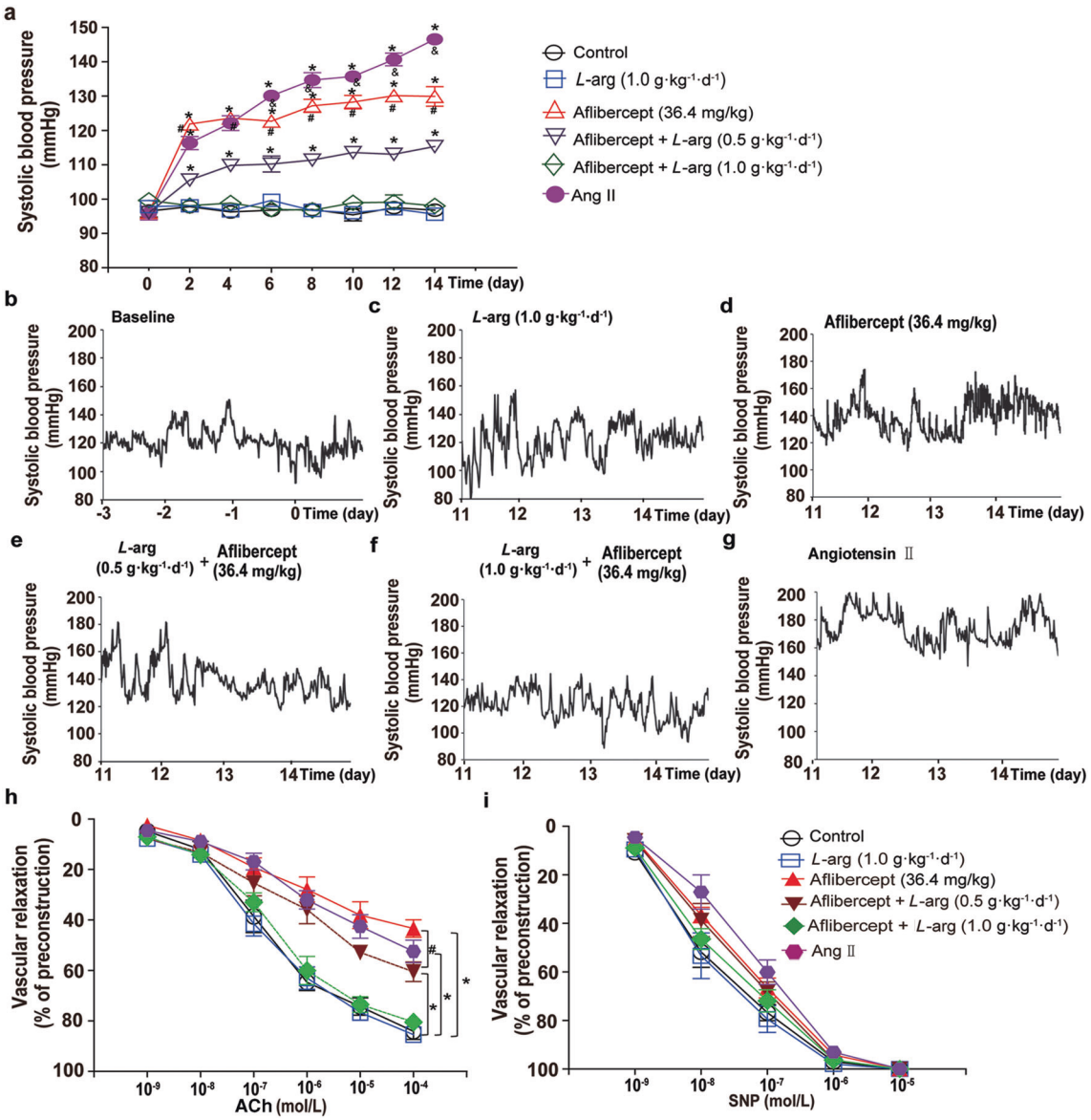

Fig. 5 Long-term application of aflibercept-induced hypertension and vascular dysfunction in mice. a The SBP of each group was measured by the noninvasive tail-cuff method for up to 14 days; the data demonstrated that *L*-arg supplementation prevented the sustained increase in SBP induced by long-term aflibercept injection ($n = 7$ or 8; $^{*}P < 0.05$ versus the saline group; $^{\#}P < 0.05$ versus the aflibercept + low-dose *L*-arg group; $^{\&}P < 0.05$ versus the Ang II group). **b**–**g** Representative SBP recordings from radiotelemetric BP measurements from WT mice 3 days before aflibercept treatment as a baseline (**b**) and from those administered *L*-arg, aflibercept and *L*-arg + aflibercept showing the raw data generated on the last 3 days (**c**–**f**), with Ang II (490 ng·kg^{-1}·min^{-1}) (**g**) as a positive control ($n = 6$). **h**, **i** Dose-response curves for endothelium-dependent (**h**) and endothelium-independent relaxation (**i**) were constructed on day 14 after injection of 36.4 mg/kg aflibercept in the presence or absence of 0.5 or 1.0 g/kg *L*-arg ($n = 7$ or 8; $^{*}P < 0.05$ versus the saline group; $^{\#}P < 0.05$ versus the aflibercept + low-dose *L*-arg group). The data are presented as the mean ± SEM; *n* represents the number of samples or mice.

and thereby causes hypertension; (4) aflibercept leads to a reduction in the intracellular levels of *L*-arg, which is associated with decreased expression of CAT-1; (5) finally, the aflibercept-induced effects on vasodilation and constriction signaling and BP were significantly inhibited by *L*-arg supplement, in a dose-dependent manner. This study thus provides novel evidence that *L*-arg supplementation could be a promising approach to protect against or treat aflibercept-induced hypertension.

Targeting the VEGF pathway has been a promising strategy for treating a variety type of cancers and other disease associated with pathological neovascularization [1, 34]. Currently, blockade of the VEGF pathway can be achieved by many different means, including blocking antibodies against VEGF or its receptors, soluble decoy receptors (SDRs) that prevent VEGF from binding to its normal receptors, or tyrosine kinase inhibitors (TKIs) of VEGFRs [35]. Aflibercept, a VEGF-Trap, is a fully human SDR protein constructed by fusing the second Ig domain of human VEGFR1 and the third Ig domain of human VEGFR2 with the constant region (Fc) of human Ig IgG1 [2]. Several clinical trials have revealed that the incidence of all grade hypertension caused by aflibercept is in the range of 28%–48%, and that the incidence of grades 3–4 hypertension is 10.2%–24.1% [36–38]. Interestingly, BP elevation usually occurs within 24 h of starting VEGFI treatment, and BP decreases upon cessation of VEGFI treatment [39]. However, for those patients with preexisting hypertension, VEGFI may cause life threatening hypertensive crisis [5].

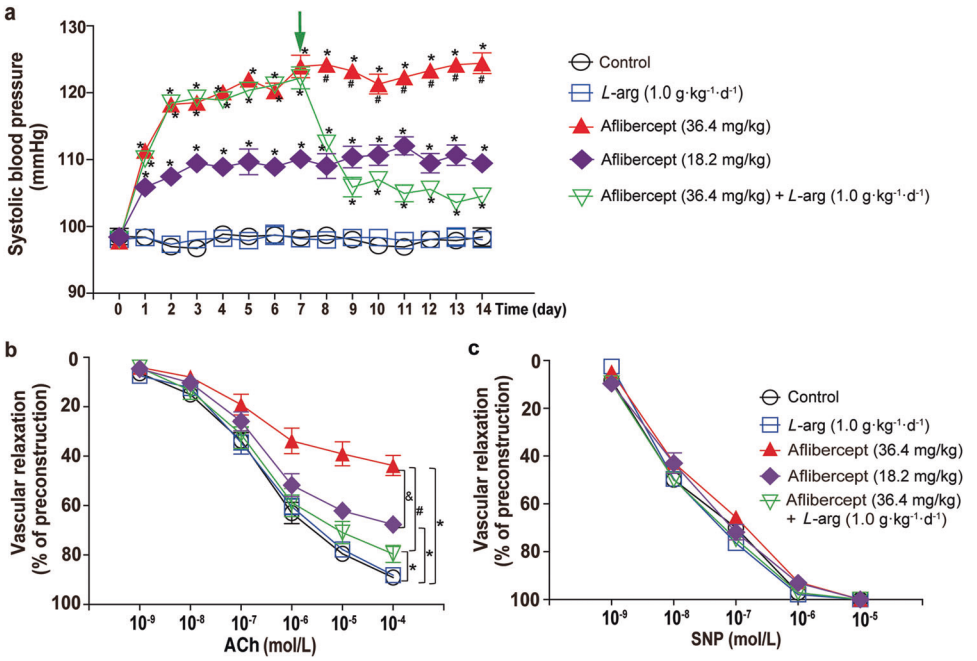

Fig. 6 ***L*-arg ameliorates hypertension and vascular dysfunction induced by long-term application of aflibercept in mice. a** The SBP of each group was measured by the noninvasive tail-cuff method for up to 14 days; consistently, long-term high-dose application of aflibercept led to a sustained increase in SBP, and this dramatic aflibercept-induced increase in SBP was greatly inhibited by *L*-arg supplementation on day 7 (as indicated by the green arrowhead) ($n = 7$; $^{*}P < 0.05$ versus the saline group; $^{\#}P < 0.05$ versus the low-dose aflibercept group). **b**, **c** Dose-response curves for endothelium-dependent (**b**) and endothelium-independent relaxation (**c**) were constructed on day 14 after injection of 36.4 mg/kg aflibercept in the presence of absence of 1.0 g/kg *L*-arg on 8–14 days ($n = 7$; $^{*}P < 0.05$ versus the saline group; $^{\#}P < 0.05$ versus the aflibercept group; $^{\&}P < 0.05$ versus the low-dose aflibercept group). The data are presented as the mean ± SEM; *n* represents the number of samples or mice.

Therefore, understanding the underlying mechanisms by which aflibercept induces hypertension is clinically significant.

Here, we revealed that a single-dose of aflibercept resulted in an acute increase in BP and impairment of EDR in response to ACh. This impairment of EDR and hypertension induced by a single dose of aflibercept-induced lasted for 4 days, albeit with a trend of decay. In contrast, long-term aflibercept also resulted in a rapid increase in BP; however, BP reached a peak rapidly and remained at a constant level. However, neither mice treated with aflibercept for a short-term nor long-term exhibited a change in vascular-wall thickness and collagen deposition, suggesting that no structural remodeling occurred during the time period of 2 weeks.

Previous studies have shown that VEGF binding to its receptors, particularly VEGFR2, results in activation of the PI3K/Akt signaling pathway and subsequently leads to the stimulation of NO release via eNOS phosphorylation [40, 41]. Unsurprisingly, we found that aflibercept, a VEGF-Trap, significantly decreased NO production by inhibiting the phosphorylationof Akt (Ser473) and eNOS (Ser1177), which resulted in impairment of EDR. On the other hand, aflibercept significantly increased the aortic ET-1 levels. A possible explanation for this result might be that the aortic ET-1 level was increased due to aflibercept-induced lack of NO bioavailability in aortic arteritis.

In addition, previous studies have demonstrated that *L*-NAME, a NO synthase inhibitor, can not only upregulate pre-pro-ET-1 mRNA, but also significantly inhibit the release of soluble endothelin converting enzyme-1, resulting in an increase in ET-1 level [42, 43]. Moreover, an increase in ET-1 level impairs endothelial NO production by inhibiting eNOS expression [44, 45]. In support of our findings, clinical and experimental studies have shown that sunitinib, a multitarget TKI of the VEGF receptor, could significantly increase circulating ET-1 levels [46].

We and others have shown that endothelial dysfunction is associated with oxidative stress [27, 47]. In this study, we observed that aflibercept significantly increased ROS and peroxynitrite generation through promoting the protein expression of NOX1 and NOX4. Consistent with our results, recent studies have shown that exposure of endothelial cells to microparticles generated from VEGF inhibitor-treated cancer patients also led to an increase in pre-pro-ET-1 mRNA expression and NADPH-dependent O_2^- generation in human aortic endothelial cells [48]. This is not surprising, because ET-1 increases the protein levels of NOX1 and NOX4 in vascular smooth muscle cells of Wistar–Kyoto rats [49]; moreover, the data from our group and others suggest that excessive accumulation of ROS might further reduce the bioavailability of NO, and may also affect eNOS expression [27, 50, 51]. Together, this evidence suggests that aflibercept induced the impairment of EDR and the increase in BP not only by reducing eNOS phosphorylation and NO production in ECs, but also by promoting ROS generation due to increasing the ET-1 levels in aortic arteries.

As a conditionally essential amino acid, *L*-arg, the substrate of eNOS, the main precursor of NO and an ET-1 suppressor [52], can also improve eNOS function by restoring eNOS phosphorylation [41, 53]. A previous study has shown that *L*-arg administration can suppress ROS generation by promoting an endogenous antioxidant response [54]. The data obtained from the present study demonstrated that the effects of aflibercept on the production of NO and ET-1, eNOS phosphorylation and NOX1/NOX4-mediated increase in the ROS generation were greatly attenuated by a high dose of *L*-arg. Importantly, a high dose of *L*-arg completely reserved the aflibercept-induced increase in BP and impairment of vascular function. Therefore, we did not perform additional experiments to test whether *L*-arg combined with antioxidative treatment could provide a better protection than *L*-arg alone. However, we cannot rule out the possibility that *L*-arg together

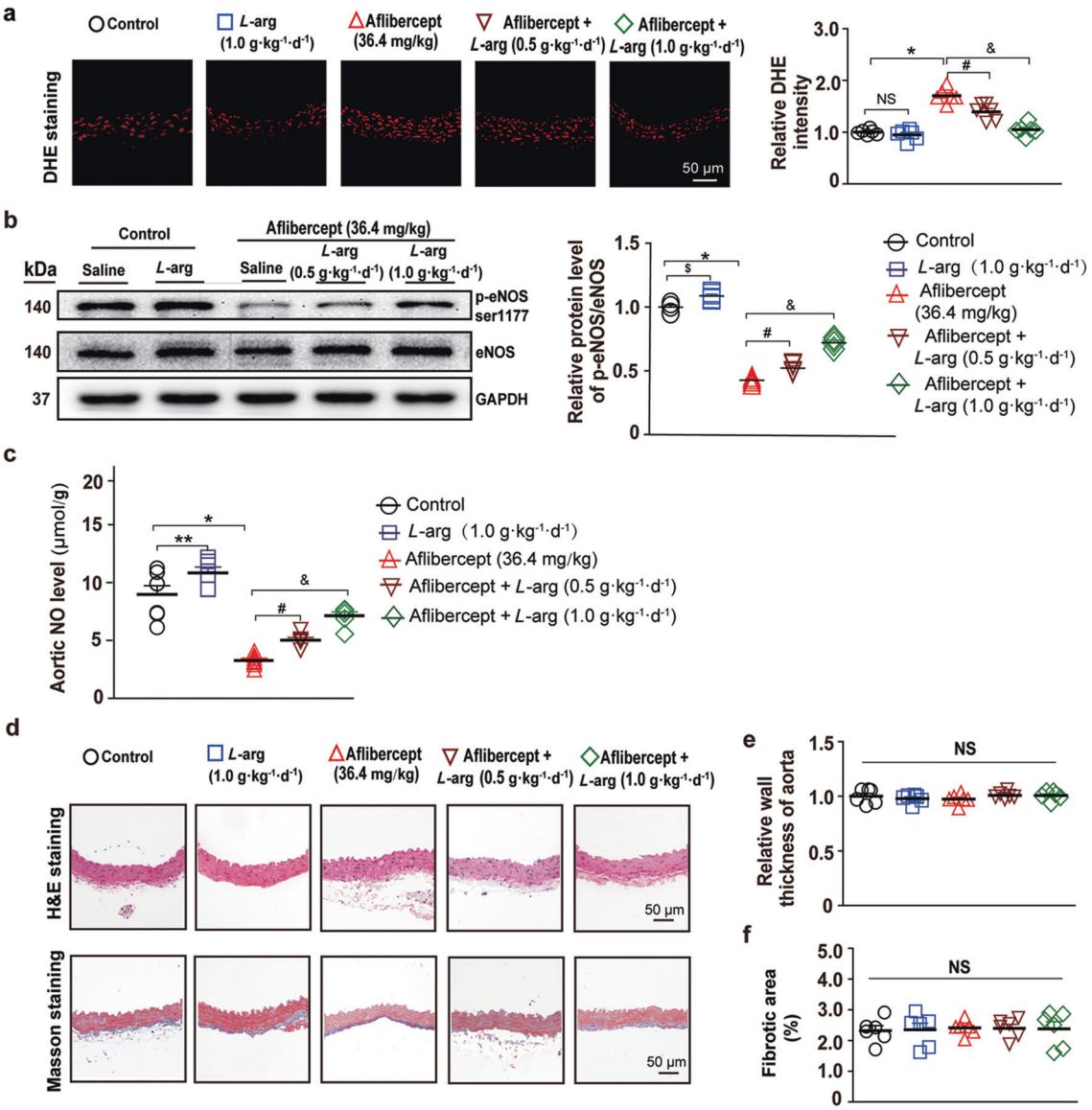

Fig. 7 *L*-arg prevents oxidative stress and the reduction in eNOS/NO signaling induced by long-term application of aflibercept. **a** Representative images of DHE staining of aortic segments after injection of a single dose of 36.4 mg/kg aflibercept in the presence or absence of *L*-arg and the fluorescence intensity data demonstrating that aflibercept-induced ROS accumulation was greatly attenuated by *L*-arg ($n = 6$; $^{*}P < 0.05$ versus the saline group; $^{\#}P < 0.05$ versus the aflibercept + low-dose *L*-arg group; $^{\&}P < 0.05$ versus the aflibercept + high-dose *L*-arg group). **b** Representative immunoblots showing p-eNOS (Ser1177) and eNOS expression in aortic tissues and quantification of protein abundance demonstrating that the aflibercept-induced decrease in p-eNOS was ameliorated by *L*-arg ($n = 4$; $^{*}P < 0.05$ versus the saline group; $^{\$}P < 0.05$ versus the *L*-arg group; $^{\#}P < 0.05$ versus the aflibercept + low-dose *L*-arg group; $^{\&}P < 0.05$ versus the aflibercept + high-dose *L*-arg group). **c** NO levels in aortic tissues were measured by the Nitric Oxide Assay Kit on day 14 in the absence or presence of *L*-arg following aflibercept injection ($n = 6$; $^{*}P < 0.05$ versus the saline group; $^{\$}P < 0.05$ versus the *L*-arg group; $^{\#}P < 0.05$ versus the aflibercept + low-dose *L*-arg group; $^{\&}P < 0.05$ versus the aflibercept + high-dose *L*-arg group). **d**–**f** Representative images of H&E staining of thoracic aortas (**d**); Wall thickness data (**e**) and the percentage of the fibrotic area in each indicated group ($n = 6$) (**f**). The data are presented as the mean ± SEM; *n* represents number of samples or mice; NS no significant difference.

with antioxidative treatment may exert a better protective effect on aflibercept-induced impairment of vascular dysfunction and hypertension. Moreover, we found that aflibercept-induced impairment of vascular relaxation and hypertension was partially reversed by high dose *L*-arg, administered 7 days after aflibercept injection. These data, along with the preventive effects of *L*-arg on aflibercept-induced hypertension, suggest that *L*-arg supplementation could be clinically significant for both the prevention and treatment of aflibercept-induced impairment of vasodilation and hypertension.

It has been reported that overexpression of soluble FMS-like tyrosine kinase 1 (sFlt-1, which prevents VEGF binding to VEGFR2) in virgin and pregnant mice significantly decreased the protein expression of CAT-1 in mice with pregnancy-associated hypertension and that administration of *L*-arg alleviated the increase in BP in sFlt-1 pregnant mice [55]. Our data showed that aflibercept led to a decrease in the expression levels of CAT-1 and intracellular *L*-arg concentration and that these effects were reversed by *L*-arg supplementation. Our results are consistent with the notion that preventing VEGF form binding to its receptor is associated with a decrease in CAT-1 expression, although the mechanisms must be further elucidated. In addition, it has been shown that treatment of the HUVECs with VEGF significantly increase CAT-1 abundance [56]. Thus, we suggest that the decreased NO bioavailability due to

the inhibition of CAT-1 may also contribute to aflibercept-induced hypertension. Furthermore, it has been shown that ROS inhibit *L*-arg transport in anococcygeus muscle [57] and that an increase in ROS may account for cyclosporine A-induced inhibition of CAT-1 protein expression. Thus we argue that ROS accumulation may also be involved in aflibercept-induced decrease in CAT-1 expression.

The best way to assess endothelial function is evaluation of the mesenteric arteries since resistant arteries are important for BP control. Because of technique limitations, we used mouse aortic arteries to examine the effects of aflibercept and *L*-arg on vasodilation function, which is a weakness of the current study. However, our results obtained from aortic arteries could indirectly reflect the relaxation of resistant artery. Nevertheless, we conclude that aflibercept causes impairment of endothelial function and hypertension, associated with inhibition of CAT-1/Akt/eNOS/NO signaling, increased ET-1 levels, and NOX1/NOX4-mediated ROS accumulation. Importantly, *L*-arg supplementation significantly attenuated and/or inhibited aflibercept-induced impairment of vascular function and hypertension by diminishing the effects of aflibercept on vasodilatation, vasoconstriction and ROS signaling. Taken together, these findings strongly suggest that *L*-arg supplementation might be a promising strategy for preventing and treating aflibercept-induced hypertension.

ACKNOWLEDGEMENTS

This work was supported by the National Natural Science Foundation of China (Grants 81870370, 81930009, and 91639202 to ZRZ), the 2017–2018 Annual Special Fund for Scientific Research and Transformation of Heilongjiang Academy of Medical Sciences (CR201810), and the Nn10 Program of Harbin Medical University Cancer Hospital.

AUTHOR CONTRIBUTIONS

ZCD, BZ, and ZRZ contributed to the conception and design of the research. ZCD, CL, YLZ, XY, CC, and XH carried out the experiments. ZCD, QSW, CL, YLZ, XY, LXZ, CC, and XH performed the data acquisition and analyzed the data. ZCD wrote the paper. BZ, MMW, and ZRZ reviewed and critically revised the paper. We are particularly grateful to Professor Hui-hua Li for his guidance and help in the experiment and paper writing. All authors read and approved the final paper and agree to be accountable for all aspects of the research in ensuring that the accuracy and integrity of all parts of the work are appropriately investigated and resolved.

ADDITIONAL INFORMATION

The online version of this article (https://doi.org/10.1038/s41401-020-00569-1) contains supplementary material, which is available to authorized users.

Competing interests: The authors declare no competing interests.

REFERENCES

1. Ferrara N, Adamis AP. Ten years of anti-vascular endothelial growth factor therapy. Nat Rev Drug Discov. 2016;15:385–403.
2. Holash J, Davis S, Papadopoulos N, Croll SD, Ho L, Russell M, et al. VEGF-Trap: a VEGF blocker with potent antitumor effects. Proc Natl Acad Sci USA. 2002;99:11393–8.
3. Rudge JS, Holash J, Hylton D, Russell M, Jiang S, Leidich R, et al. VEGF Trap complex formation measures production rates of VEGF, providing a biomarker for predicting efficacious angiogenic blockade. Proc Natl Acad Sci USA. 2007;104:18363–70.
4. Moslehi JJ. Cardiovascular toxic effects of targeted cancer therapies. N Engl J Med. 2016;375:1457–67.
5. Hamnvik OP, Choueiri TK, Turchin A, McKay RR, Goyal L, Davis M, et al. Clinical risk factors for the development of hypertension in patients treated with inhibitors of the VEGF signaling pathway. Cancer. 2015;121:311–9.
6. Gopal S, Miller KB, Jaffe IZ. Molecular mechanisms for vascular complications of targeted cancer therapies. Clin Sci. 2016;130:1763–79.
7. Belcik JT, Qi Y, Kaufmann BA, Xie A, Bullens S, Morgan TK, et al. Cardiovascular and systemic microvascular effects of anti-vascular endothelial growth factor therapy for cancer. J Am Coll Cardiol. 2012;60:618–25.
8. Touyz RM, Lang NN, Herrmann J, van den Meiracker AH, Danser AHJ. Recent advances in hypertension and cardiovascular toxicities with vascular endothelial growth factor inhibition. Hypertension. 2017;70:220–6.
9. Li W, Croce K, Steensma DP, McDermott DF, Ben-Yehuda O, Moslehi J. Vascular and metabolic implications of novel targeted cancer therapies: focus on kinase inhibitors. J Am Coll Cardiol. 2015;66:1160–78.
10. Qi WX, Shen Z, Tang LN, Yao Y. Risk of hypertension in cancer patients treated with aflibercept: a systematic review and meta-analysis. Clin Drug Invest. 2014;34:231–40.
11. Song D, Arikawa E, Galipeau DM, Yeh JN, Battell ML, Yuen VG, et al. Chronic estrogen treatment modifies insulin-induced insulin resistance and hypertension in ovariectomized rats. Am J Hypertens. 2005;18:1189–94.
12. Zhu Y, Bian Z, Lu P, Karas RH, Bao L, Cox D, et al. Abnormal vascular function and hypertension in mice deficient in estrogen receptor beta. Science. 2002;295:505–8.
13. Boese AC, Kim SC, Yin KJ, Lee JP, Hamblin MH. Sex differences in vascular physiology and pathophysiology: estrogen and androgen signaling in health and disease. Am J Physiol Heart Circ Physiol. 2017;313:H524–45.
14. Yu Q, Ma X, Wang Y, Shi HZ, An J, Wang YH, et al. Dietary cholesterol exacerbates statin-induced hepatic toxicity in syrian golden hamsters and in patients in an observational cohort study. Cardiovasc Drugs Ther. 2020. Online ahead of print.
15. Torimura T, Iwamoto H, Nakamura T, Abe M, Ikezono Y, Wada F, et al. Anti-angiogenic and antitumor activities of aflibercept, a soluble VEGF receptor-1 and -2, in a mouse model of hepatocellular carcinoma. Neoplasia. 2016;18:413–24.
16. Reagan-Shaw S, Nihal M, Ahmad N. Dose translation from animal to human studies revisited. FASEB J. 2008;22:659–61.
17. Xu X, Zhao W, Lao S, Wilson BS, Erikson JM, Zhang JQ. Effects of exercise and Larginine on ventricular remodeling and oxidative stress. Med Sci Sports Exerc. 2010;42:346–54.
18. Ohta F, Takagi T, Sato H, Ignarro LJ. Low-dose L-arginine administration increases microperfusion of hindlimb muscle without affecting blood pressure in rats. Proc Natl Acad Sci U S A. 2007;104:1407–11.
19. Gorfien S, Spector A, DeLuca D, Weiss S. Growth and physiological functions of vascular endothelial cells in a new serum-free medium (SFM). Exp Cell Res. 1993;206:291–301.
20. Deissler HL, Lang GK, Lang GE. Capacity of aflibercept to counteract VEGF-stimulated abnormal behavior of retinal microvascular endothelial cells. Exp Eye Res. 2014;122:20–31.
21. De Cilla S, Farruggio S, Cocomazzi G, Mary D, Alkabes M, Rossetti L, et al. Aflibercept and ranibizumab modulate retinal pigment epithelial cells function by acting on their cross talk with vascular endothelial cells. Cell Physiol Biochem. 2020;54:161–79.
22. Ji Y, Han Y, Diao J, Huang Y, Chen Q, Ferro A. Inhibition of endothelial nitric oxide generation by low-density lipoprotein is partially prevented by *L*-arginine and *L*-ascorbate. Atherosclerosis. 2004;176:345–53.
23. Qiu Y, Yang X, Wang L, Gao K, Jiang Z. *L*-arginine inhibited inflammatory response and oxidative stress induced by lipopolysaccharide via arginase-1 signaling in IPEC-J2 cells. Int J Mol Sci. 2019;20:1800.
24. Wang L, Li YL, Zhang CC, Cui W, Wang X, Xia Y, et al. Inhibition of Toll-like receptor 2 reduces cardiac fibrosis by attenuating macrophage-mediated inflammation. Cardiovasc Res. 2014;101:383–92.
25. Uijl E, Mirabito Colafella KM, Sun Y, Ren LW, van Veghel R, Garrelds IM, et al. Strong and sustained antihypertensive effect of small interfering RNA targeting liver angiotensinogen. Hypertension. 2019;73:1249–57.
26. Wang L, Zhao XC, Cui W, Ma YQ, Ren HL, Zhou X, et al. Genetic and pharmacologic inhibition of the chemokine receptor CXCR2 prevents experimental hypertension and vascular dysfunction. Circulation. 2016;134:1353–68.
27. Liang C, Wang QS, Yang X, Niu N, Hu QQ, Zhang BL, et al. Oxidized low-density lipoprotein stimulates epithelial sodium channels in endothelial cells of mouse thoracic aorta. Br J Pharmacol. 2018;175:1318–28.
28. Li N, Wang HX, Han QY, Li WJ, Zhang YL, Du J, et al. Activation of the cardiac proteasome promotes angiotension II-induced hypertrophy by down-regulation of ATRAP. J Mol Cell Cardiol. 2015;79:303–14.
29. Kojima H, Urano Y, Kikuchi K, Higuchi T, Hirata Y, Nagano T. Fluorescent indicators for imaging nitric oxide production. Angew Chem. 1999;38:3209–12.
30. Patel H, Chen J, Das KC, Kavdia M. Hyperglycemia induces differential change in oxidative stress at gene expression and functional levels in HUVEC and HMVEC. Cardiovasc Diabetol. 2013;12:142.
31. Collins T, Gray K, Bista M, Skinner M, Hardy C, Wang H, et al. Quantifying the relationship between inhibition of VEGF receptor 2, drug-induced blood pressure elevation and hypertension. Br J Pharmacol. 2018;175:618–30.
32. Landmesser U, Dikalov S, Price SR, McCann L, Fukai T, Holland SM, et al. Oxidation of tetrahydrobiopterin leads to uncoupling of endothelial cell nitric oxide synthase in hypertension. J Clin Invest. 2003;111:1201–9.

33. Li Q, Youn JY, Cai H. Mechanisms and consequences of endothelial nitric oxide synthase dysfunction in hypertension. J Hypertens. 2015;33:1128–36.
34. Cheung N, Lam DS, Wong TY. Anti-vascular endothelial growth factor treatment for eye diseases. BMJ. 2012;344:e2970.
35. Ellis LM, Hicklin DJ. VEGF-targeted therapy: mechanisms of anti-tumour activity. Nat Rev Cancer. 2008;8:579–91.
36. Chau I, Fakih M, Garcia-Alfonso P, Linke Z, Ruiz Casado A, Marques EP, et al. Safety and effectiveness of aflibercept + fluorouracil, leucovorin, and irinotecan (FOLFIRI) for the treatment of patients with metastatic colorectal cancer (mCRC) in current clinical practice: OZONE study. Cancers. 2020;12:657.
37. Fernandez-Martos C, Pericay C, Losa F, García-Carbonero R, Layos L, Rodríguez-Salas N, et al. Effect of aflibercept plus modified FOLFOX6 induction chemotherapy before standard chemoradiotherapy and surgery in patients with high-risk rectal adenocarcinoma: the GEMCAD 1402 randomized clinical trial. JAMA Oncol. 2019;5:1566–73.
38. Chibaudel B, Bachet JB, Andre T, Auby D, Desramé J, Deplanque G, et al. Efficacy of aflibercept with FOLFOX and maintenance with fluoropyrimidine as firstline therapy for metastatic colorectal cancer: GERCOR VELVET phase II study. Int J Oncol. 2019;54:1433–45.
39. Maitland ML, Kasza KE, Karrison T, Moshier K, Sit L, Black HR, et al. Ambulatory monitoring detects sorafenib-induced blood pressure elevations on the first day of treatment. Clin Cancer Res. 2009;15:6250–7.
40. Olsson AK, Dimberg A, Kreuger J, Claesson-Welsh L. VEGF receptor signalling—in control of vascular function. Nat Rev Mol Cell Biol. 2006;7:359–71.
41. Forstermann U, Sessa WC. Nitric oxide synthases: regulation and function. Eur Heart J. 2012;33:829–37.
42. Bourque SL, Davidge ST, Adams MA. The interaction between endothelin-1 and nitric oxide in the vasculature: new perspectives. Am J Physiol Regul Integr Comp Physiol. 2011;300:R1288–95.
43. Ahlborg G, Lundberg JM. Nitric oxide-endothelin-1 interaction in humans. J Appl Physiol. 1997;82:1593–600.
44. Ikeda U, Yamamoto K, Maeda Y, Shimpo M, Kanbe T, Shimada K. Endothelin-1 inhibits nitric oxide synthesis in vascular smooth muscle cells. Hypertension. 1997;29:65–9.
45. Ramzy D, Rao V, Tumiati LC, Xu N, Sheshgiri R, Miriuka S, et al. Elevated endothelin-1 levels impair nitric oxide homeostasis through a PKC-dependent pathway. Circulation. 2006;114:I319–26.
46. Kappers MH, van Esch JH, Sluiter W, Sleijfer S, Danser AH, van den Meiracker AH. Hypertension induced by the tyrosine kinase inhibitor sunitinib is associated with increased circulating endothelin-1 levels. Hypertension. 2010;56:675–81.
47. Higashi Y, Maruhashi T, Noma K, Kihara Y. Oxidative stress and endothelial dysfunction: clinical evidence and therapeutic implications. Trends Cardiovasc Med. 2014;24:165–9.
48. Neves KB, Rios FJ, Jones R, Evans TRJ, Montezano AC, Touyz RM. Microparticles from vascular endothelial growth factor pathway inhibitor-treated cancer patients mediate endothelial cell injury. Cardiovasc Res. 2019;115:978–88.
49. Briones AM, Tabet F, Callera GE, Montezano AC, Yogi A, He Y, et al. Differential regulation of Nox1, Nox2 and Nox4 in vascular smooth muscle cells from WKY and SHR. J Am Soc Hypertens. 2011;5:137–53.
50. Wang Y, Dong J, Liu P, Lau CW, Gao Z, Zhou D, et al. Ginsenoside Rb3 attenuates oxidative stress and preserves endothelial function in renal arteries from hypertensive rats. Br J Pharmacol. 2014;171:3171–81.
51. Kim JA, Montagnani M, Koh KK, Quon MJ. Reciprocal relationships between insulin resistance and endothelial dysfunction: molecular and pathophysiological mechanisms. Circulation. 2006;113:1888–904.
52. Kuruppu S, Rajapakse NW, Dunstan RA, Smith AI. Nitric oxide inhibits the production of soluble endothelin converting enzyme-1. Mol Cell Biochem. 2014;396:49–54.
53. Cheng H, Wang H, Fan X, Paueksakon P, Harris RC. Improvement of endothelial nitric oxide synthase activity retards the progression of diabetic nephropathy in db/db mice. Kidney Int. 2012;82:1176–83.
54. Liang M, Wang Z, Li H, Cai L, Pan JH, He HJ, et al. l-Arginine induces antioxidant response to prevent oxidative stress via stimulation of glutathione synthesis and activation of Nrf2 pathway. Food Chem Toxicol. 2018;115:315–28.
55. Shashar M, Zubkov A, Chernichovski T, Hershkovitz R, Hoffman E, Grupper A, et al. Profound decrease in glomerular arginine transport by CAT (cationic amino acid transporter)-1 contributes to the FLT-1 (FMS-like tyrosine kinase 1) induced preeclampsia in the pregnant mice. Hypertension. 2019;73:878–84.
56. Shashar M, Chernichovski T, Pasvolsky O, Levi S, Grupper A, Hershkovitz R, et al. Vascular endothelial growth factor augments arginine transport and nitric oxide generation via a KDR receptor signaling pathway. Kidney Blood Press Res. 2017;42:201–8.
57. Durlu NT, Ismailoglu UB, Sahin-Erdemli I. Inhibition of *L*-arginine transport by reactive oxygen species in rat anococcygeus muscle. Fundam Clin Pharmacol. 2003;17:609–14.